J Biol Inorg Chem (2015) 20:541–554
DOI 10.1007/s00775-015-1239-5

ORIGINAL PAPER

Synthesis, characterization and urease inhibition, in vitro anticancer and antileishmanial studies of Ni(II) complexes with *N*,*N*,*N*′-trisubstituted thioureas

Muhammad Khawar Rauf · Samad Yaseen · Amin Badshah · Sumera Zaib · Raffia Arshad · Imtiaz-ud-Din · Muhammad Nawaz Tahir · Jamshed Iqbal

Received: 11 September 2014 / Accepted: 7 January 2015 / Published online: 22 January 2015
© SBIC 2015

Abstract A series of *N*,*N*,*N*′-trisubstituted thioureas (**1–12**) and their Ni(II) complexes (**1a–12a**) were synthesized and characterized by multinuclear (^{1}H and ^{13}C) NMR, FT-IR spectroscopy and LC–MS techniques in combination with elemental analysis. The crystal structures of both ligands and Ni(II) chelates of type Ni(L-*O*, *S*)$_2$ were determined by single crystal X-ray diffraction analysis. All the complexes were adopted to have square planar geometry, where the *N*,*N*,*N*′-trisubstituted thioureas showed bidentate mode of coordination at nickel centre through oxygen and sulfur atoms. The synthesized complexes were screened for potential inhibitors of Jack bean urease. Compounds **1a** and **3a** were observed as most potent inhibitors of urease exhibiting IC_{50} values of 1.17 ± 0.12 and 1.19 ± 0.41 μM, respectively. Cytotoxicity assay on lung carcinoma (H-157) and kidney fibroblast (BHK-21) cell showed that compounds were significant anticancer agents. Additionally, the complexes were tested against *Leishmania major* and found to be potent antileishmanial agents.

Keywords *N*,*N*,*N*′-trisubstituted thioureas · Nickel(II) complexes · Urease inhibition · Anticancer · Antileishmanial

Abbreviations

ETDA	Ethylenediaminetetraacetic acid
MTT	3-(4 5-Dimethylthiazol-2-yl)-2 5-diphenyltetrazolium bromide
PBS	Phosphate-buffered saline
SRB	Sulforhodamine B
TCA	Trichloroacetic acid
TLC	Thin layer chromatography

Introduction

Thiourea derivatives are flexible ligands efficient in binding with broad range of metal ions in diverse coordination modes. Based on the number of donor functionalities in the thiourea ligand, they have potency to bind in either as monodentate or bidentate chelating fashion and in a range of protonation states as neutral ligands, or mono- or di-anions [1–3]. Thiourea ligands containing N, O and S donor atoms show a broad spectrum of biological activities, and the metal ions, bonded to bioactive compounds, may enhance/modify their activities. The substituted acyl thioureas help to establish a structure–activity relationship as certain reports manifest [4, 5]. These compounds have found extensive range of practices in heterocyclic chemistry, metal complexes and also exhibit a wide range of biological activities [6, 7]. It has been acknowledged that the activity of the metal centres toward the target bio-molecules

M. K. Rauf · S. Yaseen · A. Badshah (✉) · Imtiaz-ud-Din · J. Iqbal (✉)
Department of Chemistry, Quaid-i-Azam University, Islamabad 45320, Pakistan
e-mail: aminbadshah@yahoo.com

J. Iqbal
e-mail: drjamshed@ciit.net.pk

S. Zaib · R. Arshad · J. Iqbal
Centre for Advanced Drug Research, COMSATS Institute of Information Technology, Abbottabad 22060, Pakistan

S. Zaib
Department of Biochemistry, Hazara University, Garden Campus, Mansehra, Pakistan

M. N. Tahir
Department of Physics, University of Sargodha, Sargodha, Pakistan

can be tuned through a suitable choice of ligands. Recently, many of the acyl thioureas and their metal complexes have been screened as antitumoral, antimicrobial and enzyme inhibitors [8–11], parasiticidal [12], fungicidal, bactericidal [13] and pesticidal agents [14–16], and have shown excellent results.

Urease has a pivotal role in nitrogen metabolism of plants and microbes and acts as a virulence factor for human and animal pathogens [17–21]. It accounts for the excess quantity of ammonia and increase in pH which has negative effects in domains of agriculture and health. Urease serves as a malignant factor in microbes that are the main cause of peptic ulcers, kidney stone formation, pyelonephritis and other malfunctions [15, 16]. Urease can also decrease the effectiveness of urea fertilizers with the release of large amounts of ammonia and further enhances plant damage by ammonia toxicity and soil pH increase [17]. These adverse effects can be averted and the rate at which urea hydrolyzes using urease inhibitors that would enhance the efficiency of urea fertilizers and development of improved therapeutic strategies for the treatment of infections caused by ureolytic bacteria. Recently, urease inhibition studies for polyphenols, quinones, phosphoramides, hydroxamic acids and thiols have attracted attention to address these issues [18–31]. The inhibitory effects of metal ions upon the urease raise the possibility of metals being used as modulators and inhibitors of urease activities and this inhibition might involve blockage of thiol groups in the protein [32]. The serendipitous discovery of the metal-based drugs like antitumor-cisplatin, antileishmanial-antimonials and antirheumatic-aurafin has triggered the research in the field of inorganic medicinal chemistry. Most significant investigations on inorganic medicinal chemistry have been made to the development of anti-tumor compounds of various metals like Pt, Rh, Ru, Os, Sn, Ga, Au, Ti, Sn, Pd, Re, etc., that can exhibit improved therapeutic indexes and broader activity spectra [33–42].

The complexes of gold(I) and gold(III), palladium(II), rhenium(V), ruthenium(II), vanadium(IV) have shown great potential as inhibitors of different cysteine proteases in American trypanosomiasis and for Leishmaniasis as well [43–45]. A variety of gold(I) and gold(III) complexes have shown cytotoxic effects related to the inhibition of mitochondrial thioredoxin reductase and mitochondrial function [46–48]. In 1987, sodium aurothiomalate was used in the treatment of kala-azar and showed excellent clinical results. The gold(III), palladium(II) and rhenium(V) complexes have been tested against *Leishmania* species (*L. major*, *L. mexicana*, *L. donovani*) and *Trypanosoma cruzi*, along with evaluation of the inhibitory effect against parasite cysteine proteases. All the tested compounds were inhibitors of this parasite enzyme, and one of the palladium complexes assayed was the most active against these parasites. The preliminary data indicate that the metal complexes target parasite cysteine proteases [43, 49–51].

Baiocco et al. [52, 53] recently reported the crystal structure for Leishmania trypanothione reductase disclosing the actual mechanism of enzyme inhibition by antimonials. The observed antimony–protein interaction is consistent with the usual modalities of cysteine binding of thiophilic metals such as As(III), Sb(III) and Bi(III). Such metal-dependent inhibition of thiol reductases opens the way to combined metal therapy of parasitic diseases like leishmaniasis and the parasitic disease such as trypanosomiasis and malaria. It is very likely that this enzyme is similarly inhibited by other classes of metal complexes, like that of soft transition metals (Ni, Pd, Au, Cu, Ag, etc.). To the best of our knowledge literature related to antiparasitic studies of nickel complexes is scarcely available.

Keeping in view of the above aspects and to further explore the biological activities of acyl thiourea derivatives and their metal complexes with thiophilic metals such as nickel, palladium and platinum, we report here synthesis, characterization, urease inhibition, cytotoxicity and antileishmanial studies of nickel(II) complexes with *N*,*N*,*N*′-trisubstituted thioureas as depicted in Scheme 1.

Experimental

Materials and measurements

All reagents and solvents were purchased from commercial sources (Sigma-Aldrich Chemicals) and were used without further purification. Infrared spectra were recorded on a FT-IR IR Nicolet Avatar 320 spectrophotometer (4,000–400 cm^{-1}, KBr pellets). Elemental analyses (C, H, N, S) were carried out on a Perkin-Elmer-2400 elemental analyzer. Melting points were determined on a Kofler melting point apparatus and were uncorrected. The ^{1}H and ^{13}C NMR were recorded on a Bruker 300 MHz, internally referenced to TMS, chemical shift (δ), multiplicity (m), spin–spin coupling constant (J), integral (I). $CDCl_3$ was used as solvent, unless mentioned otherwise. LC–MS was recorded in CH_3CN solvent at ambient temperature on an Agilent 6310 ion trap instrument.

Synthesis of *N*,*N*,*N*′-trisubstituted thioureas (**1–12**)

The syntheses of *N*,*N*,*N*′-trisubstituted thiourea ligands were carried out according to the reported methodology [8–11]. To a solution of an appropriate acyl isothiocyanate (20 mmol) in acetone (30 mL) was added dropwise a solution of corresponding amine (20 mmol) dissolved in acetone with constant stirring. The reaction mixture was stirred for 8–9 h at room temperature until the reaction was

Scheme 1 The reaction scheme for the synthesis of complexes (**1a–12a**)

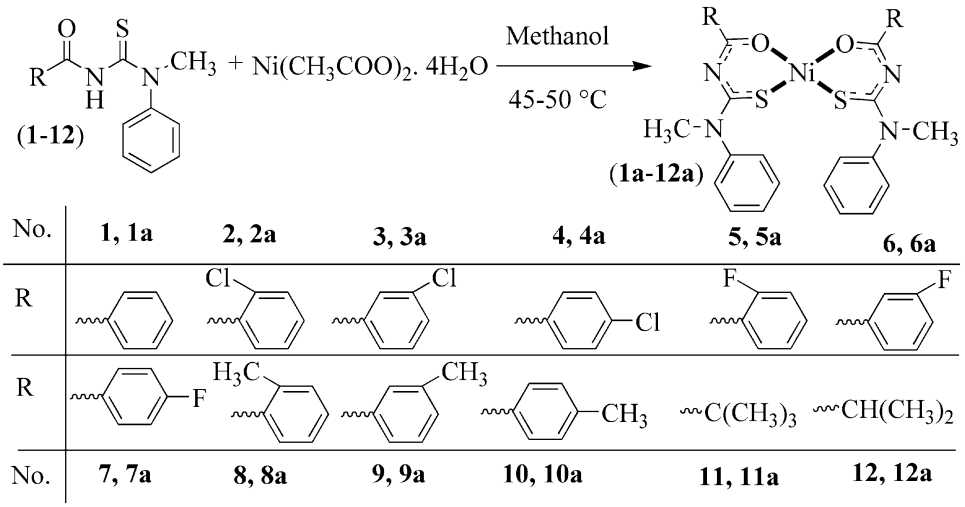

completed (the progress of the reaction was monitored by TLC). The precipitation of the pure product was done in acidified water. The solid *N*,*N*,*N*′-trisubstituted thioureas were collected by filtration and finally purified by re-crystallization from ethanol.

Synthesis of Ni(II) complexes (**1a–12a**)

A solution of the nickel acetate dihydrate (1.0 mmol), in a minimal amount of methanol, was added dropwise to a solution of the corresponding *N*,*N*,*N*′-trisubstituted thiourea (2.0 mmol), dissolved in 30 mL of methanol, at 45–50 °C. The resulting mixture was stirred for 2–4 h. The precipitated complexes were filtered and washed with dry acetone. Crystals suitable for X-ray diffraction measurements were obtained by slow evaporation of methanol/chloroform (1:1) solution of the complexes. The ^{1}H and ^{13}C NMR, FT-IR, the elemental analyses, melting point data for the ligands (**1–12**) and complexes (**1a–12a**) are as follows:

(1) *N, N*-methylphenyl-*N*′-benzoylthiourea

Yield 84 %; white solid; MP, 139.5–140.0 °C; FT-IR (KBr, cm^{-1}) 3,182 (N–H), 3,020 (C–H), 2,935 (C–H), 1,693 (C=O), 1,599, 1,513, 1,435, 1,380, 1,255, 1,167 (C=S), 1,112, 1,021, 906, 769, 708, 661, 546; ^{1}H NMR (300 MHz, $CDCl_3$) δ 3.76 (s, 3H, N–C*H*$_3$), 7.16–7.78 (m, 10H, Ar–*H*), 8.64 (s, CON*H*); ^{13}C NMR (75 MHz, $CDCl_3$) δ 45.7 (N–*C*H$_3$), 125.5, 127.5 (2C), 127.9 (2C), 128.7 (2C), 129.4 (2C), 132.7, 132.1, 145.1 (Ar–*C*), 162.8 (*C*=O), 180.7 (*C*=S); Anal. calcd. for $C_{15}H_{14}N_2OS$; C, 66.64 H, 5.22 N, 10.36 S, 11.86 Found: C, 66.63 H, 5.25 N, 10.39 S, 11.88.

(2) *N, N*-methylphenyl-*N*′-(2-chlorobenzoyl)thiourea

Yield 87 %; white solid; MP, 116–118 °C; FT-IR (KBr, cm^{-1}) 3,209 (N–H), 3,028 (C–H), 2,929 (C–H), 1,699 (C=O), 1,596, 1,518, 1,435, 1,389, 1,270, 1,242, 1,179 (C=S), 1,113, 1,048, 908, 831, 763, 746, 689, 650, 552, 464; ^{1}H NMR (300 MHz, $CDCl_3$) δ 3.74 (s, 3H, N–C*H*$_3$), 7.22–7.48 (m, 9H, Ar–*H*), 8.8 (s, CON*H*); ^{13}C NMR (75 MHz, $CDCl_3$) δ 45.3 (N–*C*H$_3$), 125.6, 126.0 (2C), 128.2, 129.7, 130.6, 130.4 (2C), 130.6, 131.2, 133.4, 142.1 (Ar–*C*), 164.6 (*C*=O), 178.8 (*C*=S); Anal. calcd. for $C_{15}H_{13}N_2OSCl$; C, 59.11 H, 4.30 N, 9.19 S, 10.52 Found: C, 59.12 H, 4.23 N, 9.21 S, 10.53.

(3) *N, N*-methylphenyl-*N*′-(3-chlorobenzoyl)thiourea

Yield 82 %; white solid; MP, 131–132 °C; FT-IR (KBr, cm^{-1}) 3,184 (N–H), 3,026 (C–H), 2,932 (C–H), 1,696 (C=O), 1,573, 1,514, 1,439, 1,389, 1,272, 1,244, 1,174 (C=S), 1,119, 1,058, 915, 763, 734, 637, 555, 466; ^{1}H NMR (300 MHz, $CDCl_3$) δ 3.77 (s, 3H, N–C*H*$_3$), 7.25–8.42 (m, 9H, Ar–*H*), 8.7 (s, CON*H*); ^{13}C NMR (75 MHz, $CDCl_3$) δ 45.6 (N–*C*H$_3$), 125.3, 125.4, 127.7 (2C), 127.8 (2C), 128.1 (2C), 129.6 (2C), 130.1, 132.5, 133.5, 134.8, 134.0 (Ar–*C*), 161.58 (*C*=O), 175.73 (*C*=S); Anal. calcd. for $C_{15}H_{13}N_2OSCl$; C, 59.11 H, 4.30 N, 9.19 S, 10.52 Found: C, 59.10 H, 4.28 N, 9.21 S, 10.50.

(4) *N, N*-methylphenyl-*N*′-(4-chlorobenzoyl)thiourea

Yield 83 %; white solid; MP, 127–129 °C; FT-IR (KBr, cm^{-1}) 3,172 (N–H), 3,071 (C–H), 2,941 (C–H), 1,698 (C=O), 1,592, 1,515, 1,428, 1,375, 1,316, 1,251, 1,181 (C=S), 1,108, 1,099, 911, 834, 743, 752, 696, 541, 471, 412; ^{1}H NMR (300 MHz, $CDCl_3$) δ 3.76 (s, 3H, N–C*H*$_3$), 7.30–7.51 (m, 9H, Ar–*H*), 8.46 (s, CON*H*); ^{13}C NMR (75 MHz, $CDCl_3$) δ 45.6 (N–*C*H$_3$), 125.1, 128.2 (2C), 129.1 (2C), 129.1 (2C), 129.4 (2C), 133.6, 139.0, 145.1 (Ar–*C*), 162.8 (*C*=O), 180.2 (*C*=S); Anal. calcd. for $C_{15}H_{13}N_2OSCl$; C, 59.11 H, 4.30 N, 9.19 S, 10.52 Found: C, 59.15 H, 4.26 N, 9.26 S, 10.50.

(5) *N, N*-methylphenyl-*N*′-(2-flourobenzoyl)thiourea

Yield 83 %; white solid; MP, 129–130 °C; FT-IR (KBr, cm^{-1}) 3,183 (N–H), 3,071 (C–H), 2,942 (C–H), 1,693(C=O), 1,592, 1,513, 1,428, 1,376, 1,318, 1,253, 1,181 (C=S), 1,108, 1,091, 913, 834, 747, 752, 695, 547,

473, 413; ^{1}H NMR (300 MHz, $CDCl_3$) δ 3.76 (s, 3H, N–CH_3), 7.32–7.57 (m, 9H, Ar–*H*), 8.57 (s, CON*H*); ^{13}C NMR (75 MHz, $CDCl_3$) δ 45.8 (N–*C*H_3),125.2, 128.1 (2C), 129.6 (2C), 129.9 (2C), 129.5 (2C), 133.1, 139.8, 145.6 (Ar–*C*), 162.4 (*C*=O), 180.0 (*C*=S); Anal. calcd. for $C_{15}H_{13}N_2OSF$; C, 62.48 H, 4.54 N, 9.72 S, 11.12 Found: C, 62.46 H, 4.55 N, 9.75 S, 11.13.

(6) *N, N*-methylphenyl-*N*′-(3-flourobenzoyl)thiourea

Yield 85 %; white solid; MP, 127–129 °C; FT-IR (KBr, cm^{-1}) 3,176 (N–H), 3,073 (C–H), 2,949 (C–H), 1,698 (C=O), 1,599, 1,513, 1,420, 1,379, 1,311, 1,258, 1,195 (C=S), 1,108, 1,094, 918, 834, 749, 751, 697, 548, 475, 412; ^{1}H NMR (300 MHz, $CDCl_3$) δ 3.78 (s, 3H, N–CH_3), 7.34–7.57 (m, 9H, Ar–*H*), 8.57 (s, CON*H*); ^{13}C NMR (75 MHz, $CDCl_3$) δ 45.3 (N–*C*H_3), 125.6, 128.1 (2C), 129.6 (2C), 129.9 (2C), 129.0 (2C), 133.2, 138.0, 147.0 (Ar–*C*), 163.7 (*C*=O), 181.1 (*C*=S); Anal. calcd. for $C_{15}H_{13}N_2OSF$; C, 62.48 H, 4.54 N, 9.72 S, 11.12 Found: C, 62.49 H, 4.50 N, 9.74 S, 11.12.

(7) *N, N*-methylphenyl-*N*′-(4-flourobenzoyl)thiourea

Yield 89 %; white solid; MP, 126–129 °C; FT-IR (KBr, cm^{-1}) 3,172 (N–H), 3,071 (C–H), 2,943 (C–H), 1,690 (C=O), 1,598, 1,511, 1,428, 1,379, 1,316, 1,254, 1,155 (C=S), 1,101, 1,099, 911, 837, 747, 752, 695, 547, 473, 413; ^{1}H NMR (300 MHz, $CDCl_3$) δ 3.77 (s, 3H, N–CH_3), 7.31–7.50 (m, 9H, Ar–*H*), 8.47 (s, CON*H*); ^{13}C NMR (75 MHz, $CDCl_3$) δ 45.6 (N–*C*H_3),125.0, 127.0 (2C), 128.0 (2C), 128.3 (2C), 129.1 (2C), 135.2, 137.0, 147.0 (Ar–*C*), 161.7 (*C*=O), 176.1 (*C*=S); Anal. calcd. for $C_{15}H_{13}N_2OSF$; C, 62.48 H, 4.54 N, 9.72 S, 11.12 Found: C, 62.47 H, 4.52 N, 9.73 S, 11.11.

(8) *N, N*-methylphenyl-*N*′-(2-methylbenzoyl)thiourea

Yield 86 %; white solid; MP, 126–127 °C; FT-IR (KBr, cm^{-1}) 3,177 (N–H), 3,093 (C–H), 2,993 (C–H), 1,660 (C=O), 1,591, 1,524, 1,439, 1,367, 1,327, 1,254, 1,178 (C=S), 1,119, 1,080, 917, 845, 758, 763, 686, 558, 494, 423; ^{1}H NMR (300 MHz, $CDCl_3$) δ 2.45 (s, 3H, –CH_3), 3.47 (s, 3H, N–CH_3), 6.31–7.70 (m, 9H, Ar–*H*), 8.40 (s, CON*H*); ^{13}C NMR (75 MHz, $CDCl_3$) δ, 29.0 (*C*H_3), 44.7 (N–*C*H_3),127.4, 129.0 (2C), 130.0 (2C), 132.3 (2C), 135.5 (2C), 137.2, 142.0, 149.0 (Ar–*C*), 167.7 (*C*=O), 185.1 (*C*=S); Anal. calcd. for $C_{16}H_{16}N_2OS$; C, 67.58 H, 5.67 N, 9.85 S, 11.28 Found: C, 67.57 H, 5.67 N, 9.86 S, 11.27.

(9) *N, N*-methylphenyl-*N*′-(3-methylbenzoyl)thiourea

Yield 88 %; white solid; MP, 128–129 °C; FT-IR (KBr, cm^{-1}) 3,191 (N–H), 3,063 (C–H), 3,001 (C–H), 1,694 (C=O), 1,583, 1,514, 1,449, 1,378, 1,327, 1,259, 1,174 (C=S), 1,108, 1,091, 922, 834, 747, 751, 690, 540, 471, 409; ^{1}H NMR (300 MHz, $CDCl_3$) δ 2.55 (s, 3H, –CH_3), 3.76 (s, 3H, N–CH_3), 6.33–7.55 (m, 9H, Ar–*H*), 8.27 (s, CON*H*); ^{13}C NMR (75 MHz, $CDCl_3$) δ, 29.9 (*C*H_3), 43.7 (N–*C*H_3),124.4, 127.0 (2C), 128.0 (2C), 129.3 (2C), 130.5 (2C), 137.2, 139.0, 144.0 (Ar–*C*), 166.7 (*C*=O), 183.1 (*C*=S); Anal. calcd. for $C_{16}H_{16}N_2OS$; C, 67.58 H, 5.67 N, 9.85 S, 11.28 Found: C, 67.56 H, 5.66 N, 9.86 S, 11.27.

(10) *N, N*-methylphenyl-*N*′-(4-methylbenzoyl)thiourea

Yield 90 %; white solid; MP, 129–130 °C; FT-IR (KBr, cm^{-1}) 3,181 (N–H), 3,077 (C–H), 2,999 (C–H), 1,676 (C=O), 1,583, 1,524, 1,428, 1,378, 1,337, 1,274, 1,168 (C=S), 110, 1,091, 916, 845, 798, 713, 656, 538, 484, 463; ^{1}H NMR (300 MHz, $CDCl_3$) δ 2.55 (s, 3H, –CH_3), 3.47 (s, 3H, N–CH_3), 6.78–7.50 (m, 9H, Ar–*H*), 8.17 (s, CON*H*); ^{13}C NMR (75 MHz, $CDCl_3$) δ, 28.9 (*C*H_3),45.9 (N–*C*H_3),125.2, 128.6 (2C), 131.0 (2C), 132.3 (2C), 133.5 (2C), 134.2, 139.0, 148.0 (Ar–*C*), 168.7 (*C*=O), 186.1 (*C*=S); Anal. calcd. for $C_{16}H_{16}N_2OS$; C, 67.58 H, 5.67 N, 9.85 S, 11.28 Found: C, 67.55 H, 5.65 N, 9.87 S, 11.27.

(11) *N, N*-methylphenyl-*N*′-pivaloylthiourea

Yield 87 %; white solid; MP, 135–137 °C; FT-IR (KBr, cm^{-1}) 3,290 (N–H), 3,072 (C–H), 3,021 (C–H), 1,667 (C=O), 1,583, 1,524, 1,428, 1,397, 1,337, 1,244, 1,171 (C=S), 1,119, 1,080, 911, 834, 746, 733, 686, 546, 478, 453; ^{1}H NMR (300 MHz, $CDCl_3$) δ, 1.34 (s, 9H, –CH_3), 3.67 (s, 3H, N–CH_3), 7.01–7.40 (m, 5H, Ar–*H*), 8.27 (s, CON*H*); ^{13}C NMR (75 MHz, $CDCl_3$) δ, 28.0 (–*C*H_3), 39.6 (*quat-C*), 42.7 (N–*C*H_3), 123.4, 125.0 (1C), 128.0 (1C), 129.3 (1C), 129.5 (1C), 135.2, 138.0, 142.0 (Ar–*C*), 161.7 (*C*=O), 183.1 (*C*=S); Anal. calcd. for $C_{13}H_{18}N_2OS$; C, 62.37 H, 7.25 N, 11.19 S, 12.81 Found: C, 62.36 H, 7.23 N, 11.21 S, 12.79.

(12) *N, N*-methylphenyl-*N*′-isobutyrylthiourea

Yield 89 %; white solid; MP, 139–141 °C; FT-IR (KBr, cm^{-1}) 3,181 (N–H), 3,083 (C–H), 3,039 (C–H), 1,663 (C=O), 1,573, 1,517, 1,427, 1,337, 1,337, 1,274, 1,187 (C=S), 1,100, 1,070, 922, 833, 747, 743, 676, 540, 470, 443; ^{1}H NMR (300 MHz, $CDCl_3$) δ, 1.18 (d, 6H, –CH_3), 2.77 (m, IH, –C*H*), 3.67 (s, 3H, N–CH_3), 7.21–7.60 (m, 5H, Ar–*H*), 8.27 (s, CON*H*); ^{13}C NMR (75 MHz, $CDCl_3$) δ 21.0 (–*C*H_3), 35.3 (*ter-C*), 44.7 (N–*C*H_3), 127.4, 130.0 (1C), 132.0 (1C), 133.3 (1C), 134.5 (1C), 137.2, 139.0, 148.0 (Ar–*C*), 164.7 (*C*=O), 187.1 (*C*=S); Anal. calcd. for $C_{12}H_{16}N_2OS$; C, 60.99 H, 6.82 N, 11.85 S, 13.57 Found: C, 60.97 H, 6.81 N, 11.87 S, 13.56.

(1a) *cis*-bis[*N,N*-methylphenyl-*N*′-benzoylthioureato-κ^2 *O,S*]nickel(II)

Yield 77 %; reddish pink solid; MP, 224–226 °C; FTIR (cm^{-1}): 3,050 (C–H), 2,939 (C–H), 1,585 (C=O), 1,511, 1,490, 1,413, 1,371, 1,270, 1,106 (C=S), 1,070, 688, 464, 402. ^{1}H NMR (300 MHz, $CDCl_3$) δ 3.63 (s, 6H, N–CH_3), 7.21-7.72 (m, 20H, Ar*H*). ^{13}C NMR (75 MHz, $CDCl_3$) δ 33.4 (N–*C*H_3), 113.5, 117.5, 127.5, 128.8, 129.3, 129.6, 136.5, 149.4, 167.6 (*C*=O), 175.1 (*C*=S). LC–MS (EI) *m/z*: 596.2 (M^+), 595.6, 433.4, 293.6 (base peak), 150.9. Anal. Calc. For $C_{30}H_{26}N_4NiO_2S_2$: C, 60.32; H, 4.39; N, 9.38; S, 10.74; Found: C, 60.35; H, 4.37; N, 9.40; S, 10.71.

(2a) *cis*-bis[(*N,N*-methylphenyl-*N*′-(2-chlorobenzoyl) thioureato-κ^2 *O,S*]nickel(II)

Yield 89 %; pink; MP, 216–218 °C; FT-IR (KBr, cm^{-1}) 3,047 (C–H), 2,925 (C–H), 1,589 (C=O), 1,569, 1,514, 1,490, 1,409, 1,374, 1,277, 1,112 (C=S), 909, 786, 658, 562, 454, 402; ^{1}H NMR (300 MHz, $CDCl_3$) δ 3.52(s, 6H, N–C*H*$_3$), 7.02-7.82 (m, 18H, Ar*H*). ^{13}C NMR (75 MHz, $CDCl_3$) δ 42.25 (N–*C*H$_3$), 126.3, 127.3, 128.2, 128.9, 129.7, 130.6, 134.8, 138.1, 145.7, 171.5 (*C*=O), 175.3 (*C*=S); LC–MS (EI) *m*/*z*: 666.2 (M^+), 631.4, 550.2, 477.4, 368.4, 327.5 (base peak), 220.1, 150.1; Anal. Calcd. for $C_{30}H_{24}Cl_2N_4NiO_2S_2$; C, 54.08 H, 3.63 N, 8.41 S, 9.63 Found: C, 54.09 H, 3.64 N, 8.42 S, 9.62.

(3a) *cis*-bis[*N,N*-methylphenyl-*N*′-(3-chlorobenzoyl) thioureato-κ^2 *O,S*]nickel(II)

Yield 78 %; reddish pink solid; MP, 234–236 °C, FTIR (cm^{-1}): 3,063 (C–H), 3,022 (C–H), 1,596 (C=O), 1,518, 1,467, 1,408, 1,371, 1,220, 1,179, 1,135 (C=S), 1,068, 901, 828, 799, 674, 555, 452, 402. ^{1}H NMR (300 MHz, $CDCl_3$) δ 3.66 (s, 6H, N–C*H*$_3$), 7.19–7.67 (m, 18H, Ar*H*). ^{13}C NMR (75 MHz, $CDCl_3$) δ 33.4 (N–*C*H$_3$), 114.2, 119.1, 125.9, 131.0, 138.3, 145.8, 152.6, 171.0 (*C*=O), 179.9 (*C*=S). LC–MS (EI) (*m*/*z*): 667.2 (M^+), 631.4 (base peak), 550.2, 477.4, 368.4, 327.5, 220.1, 150.1. Anal. Calc. For $C_{30}H_{24}Cl_2N_4NiO_2S_2$: C, 54.08; H, 3.63; N, 8.41; S, 9.63; Found: C, 54.10; H, 3.65; N, 8.43; S, 9.61.

(4a) *cis*-bis[*N,N*-methylphenyl-*N*′-(4-chlorobenzoyl) thioureato-κ^2 *O,S*]nickel(II)

Yield 75 %; reddish pink solid; MP, 244–246 °C, FTIR (cm^{-1}): 3,060 (C–H), 2,961 (C–H), 1,577 (C=O), 1,540, 1,489, 1,418, 1,373, 1,270, 1,168, 1,141 (C=S), 1,013, 905, 845, 752, 629, 578, 454, 405. ^{1}H NMR (300 MHz, $CDCl_3$) δ 3.63 (s, 6H, N–C*H*$_3$), 7.21–7.59 (m, 18H, Ar*H*). ^{13}C NMR (75 MHz, $CDCl_3$) δ 33.0 (N–*C*H$_3$), 112.9, 126.3, 127.3, 129.8, 130.6, 134.8, 138.1, 145.7, 171.5 (*C*=O), 175.3 (*C*=S). LC–MS (EI) *m*/*z*: 667.3 (M^+), 631.1, 551.0, 477.3, 367.42, 327.4 (base peak), 220.8, 150.3. Anal. Calc. For $C_{30}H_{24}Cl_2N_4$ Ni O_2S_2: C, 54.08; H, 3.63; N, 8.41; S, 9.63; Found: C, 54.12; H, 3.66; N, 8.44; S, 9.59.

(5a) *cis*-bis[*N,N*-methylphenyl-*N*′-(2-flourobenzoyl) thioureato-κ^2 *O,S*]nickel(II)

Yield 75 %; reddish pink solid; MP, 226–228 °C; FTIR (cm^{-1}): 3,066 (C–H), 2,978 (C–H), 1,584 (C=O), 1,520, 1,492, 1,410, 1,373, 1,270, 1,115 (C=S), 1,016, 908, 756, 569, 454, 403. ^{1}H NMR (300 MHz, $CDCl_3$) δ 3.50 (s, 6H, N–C*H*$_3$), 6.93–7.39 (m, 18H, Ar*H*). ^{13}C NMR ($CDCl_3$) (ppm): 31.0 (N–*C*H$_3$), 116.3, 120.3, 124.1, 128.3, 132.2, 158.4, 170.7 (*C*=O), 178.8 (*C*=S). LC–MS (EI) *m*/*z*: 633.2 (M^+), 599.3, 553.5, 452.3, 414.2, 373.2, 311.2 (base peak), 150.0. Anal. Calc. For $C_{31}H_{27}F_2N_4NiO_2S_2$: C, 57.42; H, 4.20; N, 8.64; S, 9.89; Found: C, 57.43; H, 4.23; N, 8.66; S, 9.90.

(6a) *cis*-bis[*N,N*-methylphenyl-*N*′-(3-flourobenzoyl) thioureato-κ^2 *O,S*]nickel(II)

Yield 75 %; reddish pink solid; MP, 236–238 °C; FTIR (cm^{-1}): 3,051 (C–H), 2,970 (C–H), 1,597 (C=O), 1,519, 1,492, 1,371, 1,301, 1,275, 1,117 (C=S), 1,020, 909, 763, 559, 460, 404. ^{1}H NMR (300 MHz, $CDCl_3$) δ 3.65 (s, 6H, N–C*H*$_3$), 7.21–7.92 (m, 18H, Ar*H*). ^{13}C NMR (75 MHz, $CDCl_3$) δ 31.0 (N–*C*H$_3$), 114.8, 119.2, 129.4, 130.3, 134.9, 144.9, 170.1 (*C*=O), 176.2 (*C*=S). LC–MS (EI) (*m*/*z*): 633.1 (M^+), 599.0, 553.1, 451.3, 414.0, 373.8, 311.2 (base peak), 150.8. Anal. Calc. For $C_{31}H_{27}F_2N_4NiO_2S_2$: C, 57.42; H, 4.20; N, 8.64; S, 9.89; Found: C, 57.46; H, 4.24; N, 8.68; S, 9.93.

(7a) *cis*-bis[*N,N*-methylphenyl-*N*′-(4-flourobenzoyl) thioureato-κ^2 *O,S*]nickel(II)

Yield 76 %; reddish pink solid; MP, 225–227 °C; FTIR (cm^{-1}): 3,054 (C–H), 2,959 (C–H), 1,598 (C=O), 1,501, 1,417, 1,368, 1,272, 1,208, 1,148, 1,128 (C=S), 1,012, 906, 843, 756, 551, 451, 404. ^{1}H NMR (300 MHz, $CDCl_3$) δ 3.64 (s, 6H, N–C*H*$_3$), 6.89–7.67 (m, 18H, Ar*H*). ^{13}C NMR (75 MHz, $CDCl_3$) δ 31.0 (N–*C*H$_3$), 114.9, 116.6, 127.9, 129.3, 131.1, 145.0, 167.0 (*C*=O), 180.5 (*C*=S). LC–MS (EI) (*m*/*z*): 633.2 (M^+), 599.3, 553.5, 452.3, 414.2, 373.2, 311.1 (base peak), 150.6. Anal. Calc. For $C_{31}H_{27}F_2N_4NiO_2S_2$: C, 57.42; H, 4.20; N, 8.64; S, 9.89; Found: C, 57.44; H, 4.22; N, 8.68; S, 9.91.

(8a) *cis*-bis[*N,N*-methylphenyl-*N*′-(2-methylbenzoyl) thioureato-κ^2 *O,S*]nickel(II)

Yield 76 %; red solid; MP, 212–216 °C; FT-IR (KBr, cm^{-1}) 3,053 (C–H), 2,955 (C–H), 1,596 (C=O), 1,516, 1,496, 1,362, 1,282, 1,117 (C=S), 939, 748, 655, 453, 402; ^{1}H NMR (300 MHz, $CDCl_3$) δ 2.31 (s, 6H, –C*H*$_3$), 3.33 (s, 6H, N–C*H*$_3$), 6.85–7.49 (m, 18H, Ar*H*); ^{13}C NMR (75 MHz, $CDCl_3$) δ 26.6 (–*C*H$_3$), 35.4 (N–*C*H$_3$), 116.9, 119.8, 128.0, 129.4, 131.3, 134.9, 136.8, 153.6, 171.8 (*C*=O), 177.2 (*C*=S); LC–MS (EI) *m*/*z*: 625.0 (M^+), 591.9, 509.2, 446.2, 307.0 (base peak), 150.5; Anal. Calcd. for $C_{32}H_{30}N_4$ NiO_2S_2; C, 61.45 H, 4.83 N, 8.96 S, 10.25 Found: C, 61.44 H, 4.83 N, 8.97 S, 10.24.

(9a) *cis*-bis[*N, N*-methylphenyl-*N*′-(3-methylbenzoyl) thioureato-κ^2 *O,S*]nickel(II)

Yield 78 %; brick red solid; MP, 210–213 °C; FT-IR (KBr, cm^{-1}) 3,066 (C–H), 2,984 (C–H), 1,590 (C=O), 1,512, 1,491, 1,372, 1,272, 1,101 (C=S), 933, 744, 650, 454, 403; ^{1}H NMR (300 MHz, $CDCl_3$) δ 2.32 (s, 6H, –C*H*$_3$), 3.43 (s, 6H, N–C*H*$_3$), 6.95–7.69 (m, 18H, Ar*H*); ^{13}C NMR (75 MHz, $CDCl_3$) δ 24.6 (–*C*H$_3$), 33.4 (N–*C*H$_3$), 113.9, 117.8, 127.0,128.4, 129.3, 129.9, 136.8, 151.6, 170.7 (*C*=O), 178.1 (*C*=S); LC–MS (EI) *m*/*z*: 625.2 (M^+), 591.3, 509.4, 446.3, 307.2 (base peak), 150.7; Anal. Calcd. for $C_{32}H_{30}N_4$ Ni O_2S_2; C, 61.45 H, 4.83 N, 8.96 S, 10.25 Found: C, 61.42 H, 4.87 N, 8.99 S, 10.21.

(10a) *cis*-bis[*N, N*-methylphenyl-*N*′-(4-methylbenzoyl) thioureato-κ^2 *O,S*]nickel(II)

Yield 75 %; red solid; MP, 255–258 °C; FT-IR (KBr, cm^{-1}) 3,060 (C–H), 2,973 (C–H), 1,607 (C=O), 1,581, 1,488, 1,407, 1,372, 1,274, 1,102 (C=S), 903, 688, 453, 402; ^{1}H NMR (300 MHz, $CDCl_3$) δ 2.38 (s, 6H, –C*H*$_3$), 3.60 (s, 6H, N–C*H*$_3$), 7.23–7.75 (m, 18H, Ar*H*); ^{13}C NMR (75 MHz, $CDCl_3$) δ 24.3 (–*C*H$_3$), 33.4 (N–*C*H$_3$), 113.9, 117.8, 127.5, 128.8, 129.3, 129.6, 136.5, 149.6, 169.6 (*C*=O), 176.1 (*C*=S); LC–MS (EI) *m/z*: 625.4 (M^+), 591.0, 509.2, 446.9, 307.7 (base peak), 150.9; Anal. Calcd. for $C_{32}H_{30}N_4NiO_2S_2$; C, 61.45 H, 4.83 N, 8.96 S, 10.25 Found: C, 61.43 H, 4.86 N, 8.98 S, 10.27.

(11a) *cis*-bis[*N, N*-methylphenyl-*N*′-pivaloylthioureato-κ^2 *O,S*]nickel(II)

Yield 89 %; pink solid; MP, 188–189 °C; FT-IR (KBr, cm^{-1}) 3,073 (C–H), 2,978 (C–H), 1,541 (C=O), 1,491,1,410, 1,360, 1,233, 1,112 (C=S), 1,020, 760, 452, 402; ^{1}H NMR (300 MHz, $CDCl_3$) δ 2.02 (s, 18H, –C*H*$_3$), 3.34 (s, 6H, N–C*H*$_3$), 7.13–7.54 (m, 10H, Ar*H*), ^{13}C NMR (75 MHz, $CDCl_3$) δ 20.5 (–*C*H$_3$), 32.9 (*quat-C*), 36.4 (N–*C*H$_3$), 113.5, 117.5, 129.3, 149.4, 168.0 (*C*=O), 174.9 (*C*=S); LC–MS (EI) *m/z*: 557.29 (M^+), 523.3, 395.3, 314.2, 273.2 (base peak), 150.0; Anal. Calcd. for $C_{26}H_{34}N_4NiO_2S_2$; C, 56.52 H, 6.15 N, 10.05 S, 11.51 Found: C, 56.49 H, 6.19 N, 10.11 S, 11.57.

(12a) *cis*-bis[*N, N*-methylphenyl-*N*′-isobutyrylthioureato-κ^2 *O,S*]nickel(II)

Yield 77 %; pink solid; MP, 176–178 °C; FT-IR (KBr, cm^{-1}) 3,078 (C–H), 3,018 (C–H), 1,542 (C=O), 1,481, 1,412, 1,375, 1,230, 1,117 (C=S), 1,090, 769, 452, 402; ^{1}H NMR (300 MHz, $CDCl_3$) δ 1.12 (d, 12H, –C*H*$_3$), 2.67 (m, 2H, –C*H*), 3.36 (s, 6H, N–C*H*$_3$), 7.03–7.44 (m, 10H, Ar*H*); ^{13}C NMR (75 MHz, $CDCl_3$) δ 24.5 (–*C*H$_3$), 31.0 (*ter-C*), 39.4 (N–*C*H$_3$), 112.5, 116.5, 128.3, 148.4, 169.0 (*C*=O), 176.9 (*C*=S); LC–MS (EI) *m/z*: 529.2 (M^+), 495.2, 459.1, 374.3, 259.2 (base peak), 150.0; Anal. Calcd. for $C_{24}H_{30}N_4NiO_2S_2$; C, 54.46 H, 5.71 N, 10.58 S, 12.11 Found: C, 54.49 H, 5.73 N, 10.59 S, 12.07.

Crystal structure determination

Single crystals of **12, 7, 4a, 5a** and **1a** were mounted on a thin glass fiber at room temperature and the reflection data were collected on a Bruker kappa APEXII CCD diffractometer equipped with graphite mono-chromated Mo-Kα radiation (λ = 0.71, 073 Å). Data were also corrected to Lorentz and polarization effect. The structures were solved using SHELXS-97. Final refinement on F^2 was carried out by full-matrix least-squares techniques using SHELXL-97 [54]. The crystallographic data and structure refinement parameters are summarized in Table 1.

Urease inhibition assay

The synthesized compounds were screened at a concentration of 1 mM on Jack bean urease for the inhibition potencies (Table 1). Thiourea was used as a standard inhibitor in urease inhibitory assay. The indophenol method described by Weatherburn [55] was used for the determination of urease activity. The assay mixture consisted of 40 μL of buffer (100 mmol/L urea, 0.01 mol/L K_2HPO_4, 1 mmol/L EDTA and 0.01 mol/L $LiCl_2$, pH 8.2), 10 μL of enzyme (5 U/mL) and 10 μL of test compound (1 mM). The mixture was pre-incubated at 37 °C for 30 min in 96-well plates. Following the addition of 40 μL of phenol reagent (1 %, w/v phenol, 0.005 %, w/v sodium nitroprusside) and 40 μL of alkali reagent (0.5 %, w/v NaOH, 0.1 % active chloride NaOCl) to each well and after 10 min of incubation at 37 °C, the absorbance was measured at 630 nm using a Microplate reader (Bio-Tek ELx 800™, Instruments, Inc. USA). All the experiments were carried out in triplicate. For calculation of percentage inhibition following equation was used.

$$\text{Inhibition } (\%) = 100 - \left[\frac{\text{absorbance of the compounds}}{\text{absorbance of the control}}\right] \times 100$$

The results were analyzed using PRISM 5.0 (GraphPad, San Diego, CA, USA).

Cytotoxicity assay

Cell lines and cultures

Lung carcinoma (H-157), (ATCC CRL-5,802), kidney fibroblast (BHK-21), (ATCC CCL-10) and African green monkey kidney normal cell line (Vero), (ATCC CCL-81) were kept in RPMI-1,640, having heat-inactivated fetal bovine serum (10 %) glutamine (2 mM), Pyruvate (1 mM), 100 U/mL penicillin and 100 μg/mL streptomycin, in T-75 cm^2 sterile tissue culture flasks in a 5 % CO_2 incubator at 37 °C [56]. For experiment, 96-well plates were used for growing H-157, BHK-21 and Vero cells by inoculating 5×10^4 cells per 100 μL per well and plates were incubated at 37 °C for 24 h in a humidified atmosphere containing 5 % CO_2. Within 24 h, a uniform monolayer was formed which was used for experiments.

Cytotoxicity analysis by sulforhodamine B (SRB) assays

To perform cytotoxicity assay, with H-157, BHK-21 and Vero cells, a previously described method by Skehan et al. [57] was adopted with minor modifications. Briefly, cells were cultured in different 96-well plates for 24 h. The compounds in different concentrations (100, 10, 1 and 0.1 μM) were inoculated in test wells. Furthermore, positive controls (vincristine and cisplatin) were prepared in DMSO. The well containing culture media with cells having no compound or drug was taken as blank. Vero cells were treated at 100 μM

Table 1 Crystallographic data and structure refinements for compounds **7, 12, 4a, 5a** and **1a**

	(7)	**(12)**	**(4a)**	**(5a)**	**(1a)**
Formula	$C_{15}H_{13}FN_2OS$	$C_{12}H_{16}N_2OS$	$C_{30}H_{24}Cl_2N_4NiO_2S_2$	$C_{30}H_{24}F_2N_4NiO_2S_2$	$C_{30}H_{26}N_4NiO_2S_2$
FW	288.33	236.33	666.26	633.36	597.38
T (K)	296 (2)	296 (2)	296 (2)	296 (2)	296 (2)
Crystal system	Triclinic	Triclinic	Orthorhombic	Triclinic	Monoclinic
Space group	P -1	P -1	P n a 21	P -1	P 2_1/c
a (Å)	9.9822 (5)	9.4983 (3)	25.875 (4)	9.7552 (5)	9.7893 (6)
b (Å)	11.7915 (6)	9.5093 (4)	5.5815 (8)	11.4581 (4)	13.2709 (7)
c (Å)	13.6250 (6)	14.8228 (6)	21.106 (4)	13.4532 (5)	21.6483 (14)
α (°)	71.804 (2)	79.974 (2)	90.00	73.0110 (10)	90.00
β (°)	71.430 (2)	83.843 (3)	90.00	78.801 (2)	91.835 (3)
γ (°)	84.343 (2)	89.281 (2)	90.00	88.531 (2)	90.00
V (Å^3), Z	1444.21 (12), 4	1,310.75 (9), 4	3,048.16, 4	1,409.96 (10), 2	2,810.95, 4
D_C (Mg/m^3)	1.326	1.198	1.452	1.492	1.412
μ (mm^{-1})	0.231	0.229	0.983	0.885	0.874
F(000)	600	504	1,368	652	1,240
Crystal size(mm^3)	0.40 × 0.28 × 0.26	0.38 × 0.26 × 0.22	0.30 × 0.16 × 0.14	0.32 × 0.18 × 0.16	0.35 × 0.26 × 0.20
θ range (°)	1.652–26.00	1.403–26.00	1.574–26.00	1.614–26.00	1.80–26.00
Index ranges	$-12 \le h \le 12$ $-14 \le k \le 13$ $-16 \le l \le 16$	$-11 \le h \le 11$ $-11 \le k \le 11$ $-18 \le l \le 18$	$-25 \le h \le 31$ $-4 \le k \le 6$ $-23 \le l \le 26$	$-12 \le h \le 11$ $-13 \le k \le 14$ $-11 \le l \le 16$	$-12 \le h \le 12$ $-14 \le k \le 16$ $-26 \le l \le 26$
Total reflections	20,365	18,547	12,368	17,252	22,792
Indept. Reflect. [R(int)]	5,614 (0.0301)	5,099 (0.0951)	5,387 (0.0739)	5,477(0.0265)	5,522 (0.0362)
Completeness to $\theta = 25.00°$	98.8 %	99.1 %	99.9 %	98.8 %	99.9 %
Max. and min. transmission	0.942 and 0.913	0.951 and 0.918	0.875 and 0.757	0.869 and 0.827	0.8447 and 0.7497
Data/restraints/parameters	5,614/0/364	5,099/0/296	5,387/1/337	5,477/0/372	5,522/0/354
Goodness-of-fit on F^2	1.038	1.032	0.960	1.024	1.017
Final R indices [$I > 2\sigma(I)$]	$R_1 = 0.0367$, $wR_2 = 0.0965$	$R_1 = 0.0572$, $wR_2 = 0.1070$	$R_1 = 0.0572$, $wR_2 = 0.0833$	$R_1 = 0.0317$, $wR_2 = 0.0703$	$R_1 = 0.0363$, $wR_2 = 0.0828$
R indices (all data)	$R_1 = 0.0476$, $wR_2 = 0.1057$	$R_1 = 0.1696$, $wR_2 = 0.1331$	$R_1 = 0.1291$, $wR_2 = 0.1047$	$R_1 = 0.0483$, $wR_2 = 0.0776$	$R_1 = 0.0591$, $wR_2 = 0.0952$
Largest peak and hole (e Å^{-3})	0.305 and −0.343	0.375 and −0.270	0.436 and −0.331	0.267 and −0.221	0.275 and −0.178

test compounds to check the toxicity against normal cell lines. The plates were then incubated for 48 h. After that, cells were fixed with 50 µL of 50 % ice-cold trichloroacetic acid solution (TCA) and plates were incubated at 4 °C for 1 h. Subsequently, plates were washed five times with phosphate-buffered saline (PBS) and air dried. Fixed cells were further treated with 0.4 % w/v sulforhodamine B dye (prepared in 1 % acetic acid solution) and left at room temperature for 30 min. After that the plates were rinsed with 1 % acetic acid solution and allowed to dry. In order to solubilize the dye, the dried plates were treated with 10 mM Tris base solution for 10 min at room temperature. The absorbance was measured at 490 nm subtracting the background measurement at 630 nm [58]. All experiments were repeated at least three times. Results reported are the mean value of three independent experiments (±SEM) and expressed as percent inhibitions calculated by the following formula:

$$\text{Inhibition } (\%) = 100 - \left[\frac{\text{absorbance of the test compounds}}{\text{absorbance of the control}}\right] \times 100$$

In vitro antileishmanial assay

Parasite and culture

Leishmania major promastigotes were cultured at 25 ± 1 °C to logarithmic phase in D-MEM/F-12 medium (Gibco BRL)

without phenol red, supplemented by 10 % heat inactivated fetal bovine serum (FBS), 100 IU/mL penicillin and 100 μg/mL streptomycin and then washed 3 times with phosphate-buffered saline (PBS). The cells were centrifugated at 1,500 rpm, for 10 min at room temperature and re-suspended at a concentration of 2.5×10^6 parasites/mL in medium.

Antileishmanial activity assays

In vitro antileishmanial activity of the compounds was evaluated against the promastigote forms of *Leishmania major* using a MTT (3-(4,5-dimethylthiazol-2yl)-2,5-diphenyltetrazolium bromide). The MTT assay used was originally described by Mosmann [59] and later on modified by Niks and Otto [60]. A stock solution of MTT (Sigma Chemical Co., St. Louis, Mo.) was prepared by dissolving in PBS at 5 mg/mL and storing in the dark at 4 °C for up to 2 weeks before use. For the antileishmanial activity assay, 100 μL/well of the culture which contained 2.5×10^6 cells/mL promastigotes was seeded in 96-well flat-bottom plates. Then 10 μL/well from various concentrations of compounds were added to triplicate wells and plates were incubated for 72 h at 25 ± 1 °C. The well containing only 100 μL culture medium without any compound, drug or parasite, was taken as blank. Amphotericin B was used as a standard drug. At the end of incubation, 10 μL of MTT was added to each well and plates were again incubated for 3 h at 25 ± 1 °C. Enzyme reaction was then stopped by the addition of 100 μL of 50 % isopropanol and 10 % sodium dodecyl sulfate(0.1 N HCl). The plates were incubated for an additional 30 min under agitation at room temperature. Relative optical density (OD) was then measured at a wavelength of 570 nm using a 96-well microplate reader (Bio-Tek ELx 800™, Instruments, Inc. USA). The background absorbance of plates was measured at 690 nm and subtracted from 570 nm measurement. The absorbance of the formazan produced by the action of mitochondrial dehydrogenases of metabolically active cells was correlated with the number of viable cells [59, 60]. All experiments were repeated at least three times. Results reported were the mean of three independent experiments (±SEM) and expressed as per cent inhibitions calculated by the following formula:

$$\text{Inhibition } (\%) = 100 - \left[\frac{\text{absorbance of the test compounds}}{\text{absorbance of the control}}\right] \times 100$$

Results and discussion

Synthesis and spectroscopic studies

The *N,N,N′*-trisubstituted thiourea ligands (HL) afford Ni(L-*O*, *S*)$_2$ type complexes in methanol at room temperature with nickel salts. Regarding the infrared spectra, *N,N,N*-trisubstituted thioureas (**1–12**) display strong bands in the region of 1,700–1,100 cm^{-1}. The bands that center near 1,699–1,660, 1,500–1,400 and 1,195–1,155 cm^{-1}, can be attributed to absorptions of the C=O, C–N and C=S groups, respectively. The N–H stretching vibration is observed in the region 3,290–3,172 cm^{-1} as a broad band. In the Ni(L-*O*, *S*)$_2$ complexes (**1a–12a**), the C=O and C=S bands were shifted to 1,607–1,541 and 1,141–1,101 cm^{-1}, respectively. Deprotonation induces delocalization and the C=O and C=S stretching vibration frequencies decrease by ca. 110–100 and 50–55 cm^{-1}, respectively. These band shifts confirm coordination through the oxygen and sulfur atoms. A comparative absorption pattern of the complexes with the values of the free ligands demonstrate that the coordination of thiourea ligands to nickel atom has significant effect on vibrational frequencies of N–H, C–N, C=S and C=O.

The ^{1}H NMR data for the synthesized *N,N,N′*-tisubstituted thioureas (**1–12**) showed that the N*H* hydrogen resonates considerably downfield from other resonances in the spectra. The proton chemical shifts were found in range 8.17–8.80 ppm for N*H* and aromatic protons mostly appeared downfield near 6.31–8.42 ppm as multiplets. The protons associated with aliphatic groups appeared upfield at 3.47–3.78, 2.77, 2.45–2.55, 1.34 and 1.18 ppm for N–C*H*$_3$, –C*H*(CH$_3$)$_2$, C$_{aromatic}$–C*H*$_3$, –C(C*H*$_3$)$_3$ and –CH(C*H*$_3$)$_2$, respectively. The data for the synthesized Ni(II) complexes (**1a–12a**) have shown a similar pattern except the disappearance of N*H* protons, that is, the NH protons deprotonated when acyl thiourea ligands behave as bidentate chelators [8–11].

The ^{13}C NMR data revealed that all the signals, due to the unique carbons present in ligands, thioureas (**1–12**) and the complexes (**1a–12a**), are in good agreement with the proposed structures. The aromatic carbon resonances of the thioureas were assigned on the basis of signal intensities and then were compared with the reported values [8–11]. The chemical shifts of the carbons pertaining to *C*ONH and *C*SNH groups of the thioureas resonate around 161–168 and 175–187 ppm, respectively. The substituent, –*C*H$_3$, attached to aromatic ring resonate around 29 ppm whereas in case of N–*C*H$_3$ group it resolved around 45 ppm in the compounds. The distinct carbons of –*C*(CH$_3$)$_3$ and –*C*H(CH$_3$)$_2$ groups show resonances around 28, 39 and 21, 35 ppm, respectively. However, on complexation there is a slight in δ-values associated with *C*ONH and *C*SNH groups. There is a clear shift in values of *C*ONH and *C*SNH groups present in the ligand when they are coordinated with the metal as enunciated in downfield trend for *C*ONH and a slight upfield trend in *C*SNH group (~5–6 ppm in both cases) owing to the electronegative

Table 2 The intermolecular and intramolecular hydrogen bonds for compounds **12, 7, 4a, 5a** and **1a**. Hydrogen-bond geometry: distance (Å), angle (°)

D–H···*A*	*D*–H		H···*A*	*D*···*A*	*D*–H···*A*
(**12**)					
C(2)–H(2)···S(2)^{i}	0.93		2.80	3.713 (3)	168
C(10)–H(10)···O(2)^{i}	0.98		2.59	3.318 (3)	132
C(18)–H(18)···S(1)^{ii}	0.93		3.01	3.833 (3)	149
C(19)–H(19)*C*···S(1)^{ii}	0.96		3.00	3.812 (3)	143
N(1)–H(1)···O(2)^{i}	0.86		2.13	2.903 (2)	149
N(4)–H(4)*A*···O(1)	0.86		2.09	2.924 (2)	164
(**7**)					
N(1)–H(1)···S(2)	0.86	2.68		3.4519 (13)	151
N(3)–H(3)*A*···S(1)	0.86	2.62		3.3640 (13)	145
C(24)–H(24)*C*···O(2)^{i}	0.96	2.54		3.171 (2)	124
(**4a**)					
C(9)–H(9)*A*···S(1)^{i}	0.96	2.91		3.805 (12)	155
C(30)–H(30)···S(2)^{ii}	0.93	2.95		3.837 (10)	160
(**5a**)					
C(2)–H(2)*A*···F(1)^{i}	0.96	2.58		3.407 (4)	145
C(23)–H(23)···O(2)^{ii}	0.93	2.57		3.332 (3)	139
(**1a**)					
C(11)–H(11)···N(3)^{i}	0.93	2.68		3.613 (4)	176.5

Symmetry codes: (i) $x-1, y, z$; (ii) $x+1, y, z$ (**12**); (i) $-x, -y+1, -z+1$ (**7**); (i) $x, y-1, z$; (ii) $x, y+1, z$ (**4a**); (i) $-x, -y+1, -z$; (ii) $-x+1, -y+1, -z+1$ (**5a**); (i) $-x+1, y-1/2, -z+1/2$ (**1a**)

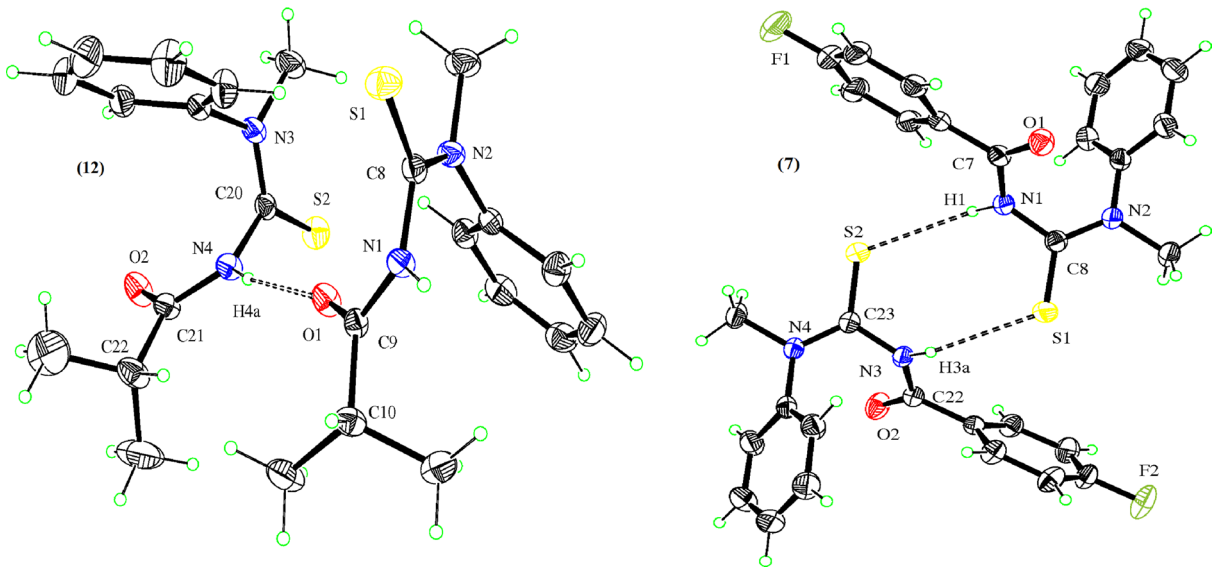

Fig. 1 ORTEP view of (**7**) and (**12**) showing 30 % probability ellipsoids. Some labels are omitted for clarity

effect of oxygen and sulfur as well as to the coordination modes the atoms.

For the *N,N,N′*-trisubstituted thiourea complexes, (CS–N) bond cleavage with the retention of charge on the thionyl group is the major fragmentation pattern noticed in these complexes, as a result of getting the [$CH_3NPh(CS)$] cation ($m/z = 150$). In the *N,N, N′*-trisubstituted thiourea complexes (**1a–12a**) retention of charge on the free ligand

Table 3 Selected bond lengths (Å) and angles (°) for compounds **12, 7, 4a, 5a** and **1a**

(12)				**(4a)**			
C(1)–C(2)	1.372 (3)	C(20)–N(4)	1.428 (3)	Ni(1)–O(1)	1.836 (6)	S(2)–C(23)	1.726 (8)
C(10)–C(12)	1.515 (4)	C(20)–S(2)	1.646 (2)	Ni(1)–O(2)	1.859 (6)	O(1)–C(1)	1.250 (9)
C(10)–C(11)	1.525 (4)	C(21)–O(2)	1.221 (2)	Ni(1)–S(1)	2.137 (3)	O(2)–C(16)	1.260 (9)
C(13)–N(3)	1.448 (3)	C(21)–N(4)	1.343 (3)	S(1)–C(8)	1.731 (9)	N(2)–C(8)	1.353 (10)
C(2)–C(1)–C(6)	120.1 (2)	C(2)–C(1)–N(2)	120.6 (2)	O(1)–Ni(1)–O(2)	84.6 (3)	S(1)–Ni(1)–S(2)	85.10 (10)
N(2)–C(8)–N(1)	116.19 (19)	N(2)–C(8)–S(1)	124.34 (17)	O(1)–Ni(1)–S(1)	95.5 (2)	C(8)–S(1)–Ni(1)	108.4 (3)
O(1)–C(9)–N(1)	122.1 (2)	O(1)–C(9)–C(10)	123.7 (2)	O(2)–Ni(1)–S(1)	179.4 (2)	C(23)–S(2)–Ni(1)	108.7 (3)
(7)				**(5a)**			
S(1)–C(8)	1.6766 (16)	S(2)–C(23)	1.6706 (16)	Ni(1)–O(2)	1.8528 (13)	N(1)–C(1)	1.345 (2)
O(1)–C(7)	1.2116 (19)	O(2)–C(22)	1.2128 (19)	Ni(1)–O(1)	1.8646 (14)	N(1)–C(3)	1.442 (3)
N(1)–C(7)	1.387 (2)	N(3)–C(22)	1.384 (2)	Ni(1)–S(2)	2.1366 (6)	N(1)–C(2)	1.467 (3)
N(2)–C(8)	1.335 (2)	N(4)–C(23)	1.336 (2)	S(1)–C(1)	1.722 (2)	N(2)–C(1)	1.344 (2)
C(7)–N(1)–C(8)	124.80 (13)	C(22)–N(3)–C(23)	123.71 (13)	S(2)–C(16)	1.7241 (19)	N(3)–C(16)	1.346 (2)
N(1)–C(7)–C(1)	114.52 (13)	N(3)–C(22)–C(16)	113.83 (13)	O(1)–C(9)	1.262 (2)	O(2)–C(24)	1.259 (2)
N(2)–C(8)–N(1)	117.11 (14)	N(4)–C(23)–N(3)	116.63 (13)	O(2)–Ni(1)–O(1)	84.02 (6)	S(2)–Ni(1)–S(1)	86.92 (2)
N(1)–C(8)–S(1)	119.23 (11)	N(3)–C(23)–S(2)	119.50 (11)	O(2)–Ni(1)–S(1)	177.70 (5)	C(9)–O(1)–Ni(1)	134.19 (13)
(1a)							
Ni(1)–O(2)	1.8535 (16)	N(1)–C(1)	1.321 (3)	O(2)–C(16)	1.260 (3)	N(4)–C(23)	1.343 (3)
Ni(1)–O(1)	1.8604 (16)	N(1)–C(8)	1.325 (3)	O(2)–Ni(1)–O(1)	84.19 (7)	S(2)–Ni(1)–S(1)	85.39 (3)
Ni(1)–S(2)	2.1325 (7)	N(2)–C(8)	1.343 (3)	O(2)–Ni(1)–S(2)	95.23 (6)	C(8)–S(1)–Ni(1)	108.59 (8)
Ni(1)–S(1)	2.1351 (7)	N(2)–C(10)	1.431 (3)	O(1)–Ni(1)–S(2)	179.17 (6)	C(23)–S(2)–Ni(1)	108.95 (8)
S(1)–C(8)	1.726 (2)	N(2)–C(9)	1.471 (3)	O(2)–Ni(1)–S(1)	178.10 (7)	C(1)–O(1)–Ni(1)	132.79 (15)
O(1)–C(1)	1.264 (3)	N(3)–C(23)	1.331 (3)	C(8)–N(2)–C(10)	124.0 (2)	C(1)–N(1)–C(8)	123.9 (2)

after the cleavage of chelate mostly gives the base peak. Comparatively low relative intensity peak was observed for the Ar–CO^+ fragment.

X-ray structure analysis

The asymmetric units of (**12**) and (**7**) contain two molecules having different conformations. The thiocarbonyl and carbonyl groups are not coplanar with the fluorophenyl ring (**12**) and isopropyl group (**7**), as reflected by the torsion angles: 122.5° for C7–N1–C8–N2, −3.6 (3)° for O1–O7–N1–C8 (**I**) and −2.2 (3)° for O2–C22–N3–C23, 58.2 (2)° for C22–N3–C23–N4 (**II**); −3.3 (2)° for O2–C21–N4–C20, 105.3 (2)° for C21–N4–C20–N3 (**I**) and 1.5 (3)° for O1–C9–N1–C8, 1.5 (3)° for C9–N1–C8–N2 (**II**), respectively. These torsion angles indicate that all the molecules have very similar conformations. The dihedral angles formed by the two benzene ring planes in (**12**) and the dihedral angles formed by the benzene ring plane and isopropyl group in (**7**) are 64.41 (5) (**I**), 87.02 (6) (**II**), and 45.32 (6) (**I**), 56.36 (**5**) (**II**), respectively, for the two molecules. The other geometric parameters present no unusual features compared with previously determined related structures. In the crystal structure of **12** intermolecular N1/4–H…O interactions connect the molecules into endless chains. The structure **7** (Fig. 1) exhibits N1/2–H…S (Table 2) bonds that link molecules into *centro*-symmetric dimmers. Crystallographic and refinement details are shown in Table 1. Selected bond lengths and angles are given in Table 3. Figure 1 shows ORTEP diagrams of [$Ni(tu)_2$] complexes **1a**, **4a** and **5a**, crystallize in monoclinic (P 2_1/c), orthorhombic (P na21) and triclinic (P -1) crystal systems, respectively. The Ni(II) cation is four-coordinated with a slight distorted square planar geometry, completed by oxygen and sulfur atoms from two thiourea ligands. Slightly distorted *cis* square planar geometry is being observed in these complexes as reflected by the angles: S1–Ni–O2 = 178.10 (6) and S2–Ni–O1 = 179.16 (6), S1–Ni–O2 = 179.4 (2) and S2–Ni–O1 = 178.8 (2), and S1–Ni–O2 = 177.70 (5) and S2–Ni–O1 = 178.93 (5), for **1a**, **4a** and **5a**, respectively. As compared to thiourea free ligand, bond lengths of C–O and C–S are relatively larger in complexes than the corresponding lengths in ligands. Other related complexes also show similar features as reported earlier [8–11]. The bond lengths of C–N in non-coordinated ligand are longer and or different than those found in the Ni(II) complexes (Fig. 2).

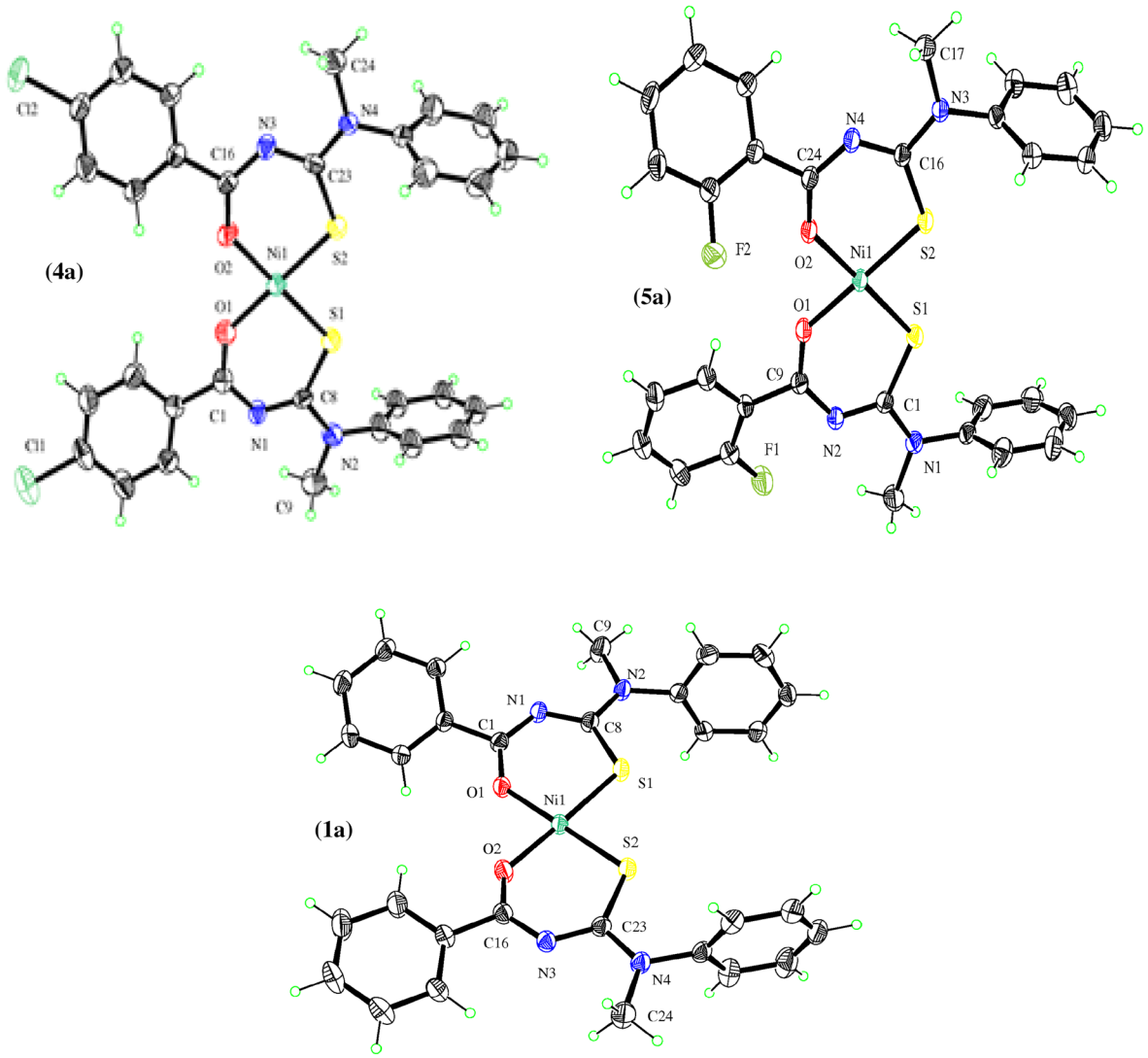

Fig. 2 ORTEP view of (**4a**), (**5a**) and (**1a**) showing 30 % probability ellipsoids. Some labels are omitted for clarity

Biological activities

Urease inhibition assay

All the synthesized Ni complexes were screened for their urease inhibitory potential. The IC_{50} values were calculated for compounds (**1–12**) and (**1a–12a**) by in vitro testing against Jack bean urease. The IC_{50} values given in the Table 4 reveal that many compounds possess potent urease inhibition. All the synthesized derivatives exhibit functional groups at phenyl ring. The screened compounds present excellent urease inhibition in micromolar range. Among the series originally designed, compound **1a** ($IC_{50} = 1.17 \pm 0.12$ μM), without any substituent in the phenyl ring, was found ~20-fold more potent as compared to thiourea ($IC_{50} = 23.0 \pm 11$ μM). Same was the case with **3a** having 3-chloro group at phenyl ring, which exhibits $IC_{50} = 1.19 \pm 0.41$ μM, ~20-fold more active than thiourea. The halogen derivatives also exhibit significant potency against urease activity. Upon further modification, moderate activity was exhibited by **2a** and **5a–10a** ranging from 3.32 to 16.4 μM. Among the synthesized analogs, **4a, 11a** and **12a** were least potent with IC_{50} values greater than 26.8 μM. In the case of *N,N,N′*-trisubstituted thioureas, compounds **1–12** show less inhibition against urease as compared to Ni complexes. The % age inhibition possessed by these compounds is shown in Table 4.

Cytotoxicity assay

Antiproliferative activity of Ni(II) complexes **1a–12a** was measured in vitro at four different concentrations (100, 10, 1 and 0.1 μM) by the cell growth inhibition against

Table 4 Urease inhibition activity of *N,N,N′*-trisubstituted thioureas (**1–12**) and Ni(II) complexes (**1a–12a**) against Jack bean urease

Compounds	% Inhibition ± SEM (μM)	Compounds	IC_{50} ± SEM (μM)
1	16.13 ± 1.23	**1a**	1.17 ± 0.12
2	15.27 ± 2.76	**2a**	2.87 ± 0.97
3	19.82 ± 2.19	**3a**	1.19 ± 0.41
4	21.95 ± 2.14	**4a**	26.8 ± 1.09
5	20.38 ± 1.45	**5a**	3.32 ± 0.73
6	25.80 ± 2.90	**6a**	8.91 ± 0.85
7	23.11 ± 1.96	**7a**	6.32 ± 0.56
8	24.67 ± 3.67	**8a**	4.53 ± 0.22
9	26.28 ± 3.21	**9a**	16.4 ± 0.16
10	27.76 ± 2.04	**10a**	13.4 ± 0.68
11	35.31 ± 3.18	**11a**	35.7 ± 2.14
12	22.65 ± 2.11	**12a**	29.1 ± 2.35
		Thiourea	23.3 ± 11.0

kidney fibroblast (BHK-21) and lung carcinoma (H157). The activity was then compared with vincristine and cisplatin, the standard anticancer drugs, to get percent inhibition of each compound. Vero cells were treated with same Ni(II) complexes **1a–12a** to find the effect of these on normal cells (Table 5). *N,N,N′*-trisubstituted thiourea compounds (**1–12**) were also tested against BHK-21 and H157 cell lines at 100 μM, and result revealed that they possess less inhibition. So the compounds were not further tested at lower concentrations.

Most of the compounds exhibited less than 50 % activity for both cell lines, having somewhat variable capacity due to their structure range in terms of attached functional groups (Table 5). Among all the screened compounds, **5a** show the highest inhibition (80.5 %) for BHK-21 cells, which is more as compared to standard drugs, vincristine (74.5 %) and cisplatin (79.5 %) at 100 μM concentrations. The compounds **6a** and **9a** proved to be potent inhibitors for cancer therapy and when were tested against BHK-21 cells showed 72.6 and 67.1 % inhibition, respectively. In case of H157, from the series of Ni(II) complexes, compound **5a** was the most potent, with 85.5 % inhibition at 100 μM. Other potent inhibitors of H157 cells were **4a, 9a** and **10a,** with 70.5, 68.9 and 68.2 % inhibition, respectively. Compound **12a** showed less than 50 % activity against H157 cells. Among the series, least active compound was **11a** with inhibition value 45.3 % and 32.0 % at 100 μM for BHK-21 and H157, respectively. When the *N,N,N′*-trisubstituted thiourea compounds (**1–12**) were tested against kidney fibroblast and lung carcinoma cell lines at 100 μM, they presented less inhibition as compared to their Ni complexes. The results are shown in Table 7.

The ability of any drug to prevent or retard the spread of malignant cells determines its role in the therapy. The anticancer drugs used in chemotherapy are fundamental antiproliferative agents. The results of present work suggested that these compounds may be a good choice for treatment of cancer after in vivo and other clinical studies. However, the exact mechanism of apoptosis of the investigated compounds in cancer cells versus normal cells still has to be determined.

Table 5 Anticancer activity of Ni(II) complexes (**1a–12a**) against kidney fibroblast (BHK-21), lung carcinoma (H157) and Vero cell lines

Compounds	Percent inhibition ± SEM								
	BHK-21				H157 vero cells				
	100 μM	10 μM	1 μM	0.1 μM	100 μM	10 μM	1 μM	0.1 μM	100 μM
1a	62.1 ± 2.5	56.5 ± 2.9	54.9 ± 2.5	51.2 ± 2.4	58.4 ± 3.1	51.1 ± 2.6	43.9 ± 2.1	37.1 ± 2.3	17.5 ± 1.3
2a	53.8 ± 4.1	49.9 ± 3.7	46.3 ± 2.9	43.8 ± 2.8	54.4 ± 2.1	51.1 ± 1.8	47.5 ± 2.6	43.1 ± 2.4	14.3 ± 2.5
3a	52.3 ± 1.9	46.3 ± 3.2	43.6 ± 2.6	40.9 ± 3.1	63.8 ± 2.5	57.3 ± 3.1	53.2 ± 2.1	40.3 ± 2.7	18.2 ± 2.1
4a	58.9 ± 3.2	53.9 ± 2.8	49.7 ± 2.4	46.7 ± 2.7	70.5 ± 2.9	62.4 ± 2.4	53.8 ± 2.4	35.2 ± 2.1	16.1 ± 1.4
5a	80.5 ± 2.8	78.9 ± 2.3	75.8 ± 2.6	73.7 ± 2.4	85.5 ± 2.8	80.9 ± 2.3	77.8 ± 2.6	41.7 ± 2.4	21.3 ± 1.6
6a	72.6 ± 2.8	68.7 ± 1.8	62.0 ± 1.8	53.1 ± 2.7	51.5 ± 2.1	47.4 ± 2.4	43.4 ± 2.5	36.4 ± 2.7	19.4 ± 1.9
7a	58.4 ± 3.1	55.1 ± 2.6	51.9 ± 2.1	47.1 ± 2.3	78.6 ± 2.4	65.6 ± 3.2	52.3 ± 2.9	49.6 ± 2.1	12.6 ± 1.0
8a	56.4 ± 2.9	53.3 ± 2.5	50.3 ± 2.3	46.2 ± 3.2	56.9 ± 2.3	62.3 ± 3.0	47.8 ± 2.7	34.5 ± 3.3	17.7 ± 1.2
9a	67.1 ± 2.7	62.5 ± 2.8	55.1 ± 3.0	48.2 ± 2.2	68.9 ± 2.3	65.6 ± 3.1	61.7 ± 2.2	37.2 ± 3.0	20.2 ± 1.5
10a	57.6 ± 1.8	54.6 ± 2.9	47.2 ± 2.3	44.4 ± 2.3	68.2 ± 2.5	60.7 ± 2.7	49.9 ± 2.6	35.2 ± 1.8	14.9 ± 1.5
11a	45.3 ± 2.3	41.6 ± 2.9	27.7 ± 2.7	24.8 ± 2.4	32.0 ± 2.2	28.5 ± 1.9	25.6 ± 3.1	21.3 ± 2.1	15.7 ± 1.8
12a	56.4 ± 2.9	51.3 ± 2.5	45.3 ± 2.3	36.2 ± 3.2	49.2 ± 3.0	45.2 ± 2.7	41.4 ± 1.3	32.4 ± 2.8	18.6 ± 2.1
Vincristine	74.5 ± 2.9	72.6 ± 3.1	70.9 ± 2.4	69.8 ± 1.9	74.5 ± 2.9	72.6 ± 3.1	70.9 ± 2.4	69.8 ± 1.9	
Cisplatin	79.5 ± 1.3	76.5 ± 2.4	71.4 ± 1.8	68.3 ± 2.1	79.5 ± 1.3	76.5 ± 2.4	71.4 ± 1.8	68.3 ± 2.1	

Table 6 Antileishmanial activity of Ni(II) complexes (**1a–12a**)

Compounds	Percent Inhibition ± SEM			
	100 μM	10 μM	1 μM	0.1 μM
1a	52.5 ± 2.1	49.5 ± 2.5	46.2 ± 1.7	42.5 ± 2.0
2a	59.8 ± 1.7	56.4 ± 1.4	52.3 ± 1.8	39.3 ± 2.0
3a	53.8 ± 1.6	51.4 ± 2.5	49.1 ± 2.3	42.7 ± 1.7
4a	56.8 ± 1.8	50.0 ± 2.2	43.8 ± 1.3	36.4 ± 2.2
5a	72.6 ± 1.9	64.9 ± 1.3	52.2 ± 2.2	44.6 ± 1.5
6a	60.5 ± 2.3	57.2 ± 2.1	52.2 ± 1.4	45.6 ± 1.2
7a	56.7 ± 2.4	54.3 ± 2.1	41.6 ± 1.6	27.7 ± 2.1
8a	61.2 ± 2.3	55.9 ± 1.9	52.9 ± 1.5	43.3 ± 2.2
9a	71.4 ± 2.1	65.9 ± 2.8	58.5 ± 1.9	39.1 ± 1.3
10a	63.1 ± 2.7	57.6 ± 1.8	52.5 ± 2.1	38.6 ± 2.7
11a	38.5 ± 1.1	35.9 ± 1.7	27.2 ± 1.5	19.6 ± 1.9
12a	46.7 ± 2.4	43.6 ± 2.1	31.6 ± 1.6	27.7 ± 3.1
Amphotericin B	79.8 ± 1.8	76.3 ± 1.4	74.8 ± 2.7	69.9 ± 2.3

Table 7 % inhibition activity of *N,N,N′*-trisubstituted thioureas (**1–12**) against kidney fibroblast (BHK-21) and lung carcinoma (H157) cell lines and Leishmania major

Compounds	% Inhibition at 100 μM		
	BHK-21	H157	Leishmania
1	4.31	8.95	8.43
2	15.93	10.93	17.54
3	18.80	19.61	33.33
4	−7.26	−0.48	17.98
5	23.02	5.19	−12.67
6	−7.51	13.78	14.91
7	12.39	−8.35	−9.21
8	22.03	20.64	15.78
9	−9.22	12.95	22.80
10	12.83	9.73	6.57
11	−23.26	16.90	7.45
12	25.66	11.47	22.81

Antileishmanial assay

The antileishmanial activity of Ni(II) complexes (**1a–12a**) was measured by MTT method and the investigated compounds produce significant reduction in viable promastigotes as shown in Table 6. Amphotericin B was used as a standard drug for anti-leishmanial activity. The results in Table 6 reveal that the tested compounds show significant inhibition against *leishmania major* in a dose-dependent manner. Almost all the compounds showed remarkable in vitro antileishmanial activity when checked at different concentrations (100, 10, 1, 0.1 μM). Antileishmanial activity of the Ni(II) complexes (**1a–12a**) proved significant inhibitory potential as compared to *N,N,N′*-trisubstituted thiourea compounds (**1–12**) at 100 μM, which exhibited less inhibition as shown in Table 7.

Among all the compounds screened in the series, **5a** and **9a** show excellent inhibition comparable with Amphotericin B used as a standard drug. Compounds **6a, 8a** and **10a** also revealed significant inhibition against leishmania major. Other complexes like **1a, 2a, 3a, 4a** and **7a** also exhibited good inhibition. Least active compounds among the series were **11a** and **12a**, which displayed less than 50 % inhibition. These results may support the probable use of these compounds, as a source of advance antileishmanial agents.

Conclusions

A series of *N,N,N′*-trisubstituted thioureas (**1–12**) and their Ni(II) complexes (**1a–12a**) were synthesized. The inhibition ability of these compounds against urease was evaluated. The results presented above clearly demonstrate that *N,N,N′*-trisubstituted thioureas showed little inhibitory activity against Jack bean urease as compared to their Ni(II) complexes. The compounds **1a, 2a, 3a, 5a, 6a, 7a, 8a, 9a** and **10a** showed excellent urease inhibition, more than the standard drug. The inhibitors **1a** and **3a** were most potent having IC_{50} value 1.17 ± 0.12 and 1.19 ± 0.41 μM, respectively. Therefore, these drugs are beneficial and potential alternatives and hence should be investigated further for the control of associated diseases. In case of cytotoxic and antileishmanial activity, Ni complexes proved to have significant inhibitory potential against both the cell lines when compared to *N,N,N′*-trisubstituted thioureas. Complexes represented remarkable ability to inhibit the growth of cancer cells and had little toxic effect on normal cell lines. Moreover, complexes revealed potent inhibition against leishmaniasis. Due to synthetic and biological versatility of tested compounds, they may be used as therapeutic agents having antiproliferative and antileishmanial activities after further in vivo studies.

Supplementary data

Crystallographic data (excluding structure factors) for the structures reported in this paper have been deposited in the Cambridge Crystallographic Data Centre as supplementary publication no. CCDC-1010230 for (**7**), CCDC-1010231 for (**12**), CCDC-1010227 for (**1a**), CCDC-1010228 for (**4a**) and CCDC-1010229 for (**5a**). Copies of available materials can be obtained, free of charge, on application to the director, CCDC, 12 Union Road, Cambridge CB21EZ, UK, (Fax: +44-(0)-1223-336033 or e-mail: deposit@ccdc.cam.ac.uk).

Acknowledgments The M. Khawar Rauf is thankful to the Quaid-e-Azam University, Islamabad, Pakistan, for the grant of funds for Post-doctoral Fellowship.

References

1. Livingstone SE (1987) In: Gillard RD, McCleverty JA (eds) Comprehensive coordination chemistry. Pergamon, Oxford, p 639
2. Janakiram-Sayala C, Bosman WP, Willemse J, Cras JA (1980) Recl Trav Chim Pays-Bas 99:314–316
3. Cheresova EN, Zhukova RS, Tatarintseva TB, Cheresov SV, Mukmeneva NA (1997) Russ J Gen Chem 67(8):1271–1275
4. Beyer L, Criado JJ, Garcia E, Leβmann F, Medarde M, Richter R, Rodriguez E (1996) Tetrahedron 52:6233–6240
5. Bourne S, Koch KR (1993) J Chem Soc Dalton Trans 13:2071–2072
6. Aly AA, Ahmed EK, El-Mokadem KM, Hegazy MAF (2007) J Sulfur Chem 28:73–93
7. Aly AA, Nour-El-Din AM, Gomaa AM, Brown AB, Fahmi MS (2007) J Chem Res 439–441
8. Rauf MK, Talib A, Badshah A, Zaib S, Shoaib K, Shahid M, Flörke U, Imtiaz-ud-Din, Iqbal J (2013) Eur J Med Chem 70:487–496
9. Saeed A, Khan MS, Rafique H, Shahid M, Iqbal J (2014) Bioorg Chem 52:1–7
10. Rauf MK, Imtiaz-ud-Din, Badshah A, Gielen M, Ebihara M, Vos D, Ahmed S (2009) J Inorg Biochem 103:1135–1144
11. Gul R, Rauf MK, Badshah A, Azam SS, Tahir MN, Khan A (2014) Eur J Med Chem 85:438–449
12. Müller J, Limban C, Stadelmann B, Missir AV, Chirita IC, Chifiriuc MC, Nitulescu GM (2009) Parasitol Int 58:128–135
13. Campo R, Criado JJ, Gheorghe R, Gonzalez FJ, Hermosa MR, Sanz F, Manzano JL, Monte E, Fernandez ER (2004) J Inorg Biochem 98:1307–1314
14. Duan LP, Xue J, Xu LL, Zhang HB (2010) Molecules 15:6941–6947
15. Zhong ZM, Xing R, Liu S, Wang L, Cai SB, Li PC (2008) Carbohydr Res 343:566–570
16. Wang ZY, Wang S, Song XJ, Wang YG (2005) Chin J Pestic Sci 7:282–284
17. Karplus PA, Pearson MA, Hausinger RP (1997) Acc Chem Res 30:330–337
18. Hausinger RP (ed) (1993) Biochemistry of nickel. Plenum Press, New York
19. Mobley HLT, Hausinger RP (1989) Microbiol Rev 53:85–108
20. Mobley HLT, Island MD, Hausinger RP (1995) Microbiol Rev 59:451–480
21. Jabri E, Carr MB, Hausinger RP, Karplus PA (1995) Science 268:998–1004
22. Krajewska B (2009) J Mol Catal B Enzym 59:9–21
23. Vassiliou S, Kosikowska P, Grabowiecka A, Yiotakis A, Kafarski P, Berlicki Ł (2010) J Med Chem 53:5597–5606
24. Font M, Domínguez M-J, Sanmartín C, Palop JA, San-Francisco S, Urrutia O, Houdusse F, García-Mina JM (2008) J Agric Food Chem 56:8451–8460
25. Domínguez M-J, Sanmartín C, Font M, Palop JA, San-Francisco S, Urrutia O, Houdusse F, García-Mina JM (2008) J Agric Food Chem 56:3721–3731
26. Benini S, Rypniewski WR, Wilson KS, Ciurli S, Mangani S (2001) J Biol Inorg Chem 6:778–790
27. Benini S, Rypniewski WR, Wilson KS, Mangani S, Ciurli S (2004) J Am Chem Soc 126:3714–3715
28. Todd MJ, Hausinger RP (2000) Biochemistry 39:5389–5396
29. Vassiliou S, Grabowiecka A, Kosikowska P, Yiotakis A, Kafarski P, Berlicki Ł (2008) J Med Chem 51:5736–5744
30. Benini S, Rypniewski WR, Wilson KS, Ciurli S, Mangani S (1998) J Biol Inorg Chem 3:268–273
31. Todd MJ, Hausinger RP (1989) J Biol Chem 264:15835–15842
32. Hughes RB, Katz SA, Stubbins SE (1969) Enzymologia 36:332–334
33. Bruijnincx PCA, Sadler PJ (2008) Curr Opin Chem Biol 12:197–206
34. Storr T, Thompson KH, Orvig C (2006) Chem Soc Rev 35:534–544
35. Hambley TW (2007) Dalton Trans pp. 4929–4937
36. Allardyce CS, Dyson PJ (2006) Top Organomet Chem 17:177–210
37. Thompson KH, Orvig C (2006) Dalton Trans 761–764
38. Ronconi L, Sadler PJ (2007) Coord Chem Rev 251:1633–1648
39. Jakupec MA, Galanski M, Arion VB, Hartinger CG, Keppler BK (2008) Dalton Trans 183–194
40. Hanif M, Babak MV, Hartinger CG (2014) Drug Discov Today 19(10):1640–1648
41. Dömötör O, Aicher S, Schmidlehner M, Novak MS, Roller A, Jakupec MA, Kandioller W, Hartinger CG, Keppler BK, Enyedy EA (2014) J Inorg Biochem 134:57–65
42. Muhammad N, Guo Z (2014) Curr Opin Chem Biol 19:144–153
43. Fricker SP, Mosi RM, Cameron BR, Baird I, Zhu Y, Anastassov V, Cox J, Doyle PS, Hansell E, Lau G, Langille J, Olsen M, Qin L, Skerlj R, Wong RSY, Santucci Z, McKerrow JH (2008) J Inorg Biochem 102:1839–1845
44. Barbosa MIF, Corrêa RS, de Oliveira KM, Rodrigues C, Ellena J, Nascimento OR, Rocha VPC, Nonato FR, Macedo TS, Barbosa-Filho JM, Soares MBP, Batista AA (2014) J Inorg Biochem 136:33–39
45. Gambino D (2011) Coord Chem Rev 255:2193–2203
46. Barnard PJ, Berners-Price SJ (2007) Coord Chem Rev 251:1889–1920
47. Hickey JL, Ruhayel RA, Barnard PJ, Baker MV, Berners-Price SJ, Filipovska A (2008) J Am Chem Soc 130:12570–12571
48. Rigobello MP, Messori L, Marcon G, Bragadin M, Folda A, Scutari G, Bindoli A (2004) J Inorg Biochem 98:1634–1641
49. Navarro M, Hernández C, Colmenares I, Hernández P, Fernández M, Sierraalta A, Marchán E (2007) J Inog Biochem 101:111–116
50. Singh MP, Mishra M, Khan A, Ramdas SL, Panjiyar S (1989) Br Med J 299:1318
51. Navarro M (2009) Coord Chem Rev 253:1619–1626
52. Rosenthal PJ (2004) Int J Parasitol 34:1489–1499
53. Baiocco P, Colotti G, Franceschini S, Ilari A (2009) J Med Chem 52:2603–2612
54. Sheldrick GM (2008) Acta Crystallogr A 64:112–122
55. Weatherburn MW (1967) Anal Chem 39:971–974
56. Araki-Sasaki K, Aizawa S, Hiramoto M, Nakamura M, Iwase O, Nakata K, Sasaki Y, Mano T, Handa H, Tano Y (2000) J Cell Physiol 182:189–195
57. Skehan P, Storeng R, Scudiero D, Monks A, McMahon J, Vistica D, Warren JT, Bokesch H, Kenney S, Boyd MR (1990) J Natl Cancer Inst 82:1107–1112
58. Longo-Sorbello GS, Saydam G, Banerjee D, Bertino JR (2005) In: Celis JE, Carter N, Simons K, Small JV, Hunter T (eds) Cytotoxicity and cell growth assays. Cell biology, pp. 315–324
59. Mosmann T (1983) J Immunol Methods 65:55–63
60. Niks M, Otto M (1990) J Immunol Methods 130:149–151